Diastereoselective Arbuzov Dealkylation of Cobalt(III) Perfluoroalkyl Prochiral Phosphonite Complexes

Chet R. Jablonski,* Huaizhu Ma,[1] Zhao Chen, Rosemary C. Hynes,[2] John N. Bridson, and Monica P. Bubenik

Department of Chemistry, Memorial University, St. John's, Newfoundland A1B 3X7, Canada

Received August 14, 1992

Treatment of (η^5-Cp)Co*(PPh_2NHC*H(Me)Ph)(X)(I) (**1a**, X = CF_3; **1b**, X = C_3F_7) with dimethyl phenylphosphonite affords the corresponding Co,P-chiral phosphinate products (η^5-Cp)Co*(PPh_2NHC*H(Me)Ph)(X)(P*(O)Ph(OMe)) ($(R,S)_{Co};(R,S)_P;(S)_C$-**3**) and (η^5-Cp)Co*($PPh(OMe)_2$)(X)(P*(O)Ph(OMe)) ($(R,S)_{Co};(R,S)_P$-**6**) as a mixture of diastereomers. Absolute configurations of **3a,b** were determined by a combination of single-crystal X-ray diffraction and chiroptical (CD) data. $(-)_{436}$-$(R)_{Co};(R)_P;(S)_C$-**3a** crystallizes in the orthohombic system $P2_12_12_1$ with a = 8.7863(12) Å, b = 17.2438(19) Å, c = 21.3634(19) Å, V = 3236.8(6) Å^3, Z = 4, R_F = 6.6% (R_w = 2.7%) for 2588 reflections with $I_{net} > 2.5\sigma$. $(+)_{436}$-$(S)_{Co};(R)_P;(S)_C$-**3a** crystallizes in the trigonal system $P3_1$ with a = 14.9469(14) Å, c = 12.2911(8) Å, V = 2378.1(3) Å^3, Z = 3, R_F = 6.8% (R_w = 4.0%) for 1057 reflections with $I_{net} > 2.5\sigma$. $(-)_{436}$-$(R)_{Co};(R)_P;(S)_C$-**3b** crystallizes in the orthorhombic system $P2_12_12_1$ with a = 12.4590(14) Å, b = 16.1554(22) Å, c = 17.6204(14) Å, V = 3546.6(7) Å^3, Z = 4, R_F = 6.5% (R_w = 5.1%) for 2096 reflections with $I_{net} > 2.5\sigma$. $(-)_{436}$-$(R)_{Co};(S)_P;(S)C$-**3b**·CH_2Cl_2 crystallizes in the orthorhombic system $P2_12_12_1$ with a = 15.929(3) Å, b = 17.670(2) Å, c = 13.549(2) Å, V = 3813.6(9) Å^3, Z = 4, R_F = 6.3% (R_w = 4.7%) for 2113 reflections with $I_{net} > 3.0\sigma$. The perfluoroalkyl-substituted chiral phosphinate products are configurationally stable at cobalt and phosphorus in solution. Strong intramolecular P=O···H—N hydrogen bonding in the product phosphinate complexes **3** establishes a "chaise lounge" six-membered-ring conformation with pseudoequatorial η^5-C_5H_5 and pseudoaxial perfluoroalkyl in the solid state. Nuclear Overhauser difference (NOED) spectra demonstrate that the solid-state conformation of **3** is not substantively different from the preferred conformation in solution. Arbuzov-like dealkylation of an unobserved intermediate phosphonite complex occurs with higher Co→P chiral induction for the hydrogen-bonded methyl phenylphosphinate products **3** than for the non-hydrogen-bonded analogs **6**.

Introduction

Our previous work in this area[3] demonstrated a direct, effective chirality transfer from a pseudooctahedral, stereogenic cobalt atom to a prochiral phosphorus which can be stereoselectively dealkylated under transition-metal-mediated (TMM) Arbuzov conditions, cf. **2**→**3** (X = I). Initial investigations were complicated by the propensity of halide-substituted derivatives to epimerize at the stereogenic cobalt center; hence, we sought to prepare more stereochemically robust[4] perfluoroalkyl analogs. Herein we report our findings using the transition-metal chiral auxillary (η^5-Cp)Co(X)(PNH*) (X = CF_3, C_3F_7; PNH* = (*S*)-(−)-PPh_2NHC*H(Me)Ph).

Results and Discussion

Synthesis and Characterization of the Chiral Phosphinate Complexes. Treatment of **1a,b** (**a**, X = CF_3; **b**, X = C_3F_7) with a stoichiometric quantity of dimethyl phenylphosphonite in benzene, chloroform, or acetone solvent at ambient temperature affords two types of orange methyl phenylphosphinate products, **3** and **6**,[5] as a mixture of all possible diastereomers in relatively low conversions. Carius tube reactions at high temperature (100–120 °C) did not give improved yields. We anticipated[3] that the formation of **3** would occur by initial iodide substitution to give the cationic phosphonite complex **2**, which would subsequently dealkylate via an Arbuzov-like rearrangement.[4,6-17] ^{1}H NMR experiments, however, showed that the primary substitution product is in fact **4**, which forms via dissociation of the relatively bulky neutral aminophosphine ligand in a preequilibrium step. Addition of dimethyl phenylphosphonite to solutions of **1** at ambient temperature in chloroform solvent resulted in a rapid reaction (ca. 5 min) which afforded an equlibrium mixture containing **1**, **4**, $PPh(OMe)_2$, and $PPh_2NHCH(Me)Ph$ (K_{eq}

(1) Present address: Institute of Organic Chemistry, Anhui Normal University, Wuhu, Anhui, PRC.
(2) Present address: Chemistry Division, NRC, Ottawa, Canada K1A 0R6.
(3) Brunner, H.; Jablonski, C. R.; Jones, P. G. *Organometallics* **1988**, *7*, 1283–1292.
(4) Jablonski, C. R.; Ma, H.; Hynes, R. C. *Organometallics* **1992**, *11*, 2996–2802.
(5) Complexes in the **6a** series were characterized by comparison of NMR parameters derived from **6b**.
(6) Brill, T. B.; Landon, S. J. *J. Am. Chem. Soc.* **1982**, *104*, 6571–6575.
(7) Brill, T. B.; Landon, S. J. *Inorg. Chem.* **1964**, *23*, 4177–4181.
(8) Brill, T. B.; Landon, S. J. *Inorg. Chem.* **1984**, *23*, 1266–1271.
(9) Brill, T. B.; Landon, S. J. *Chem. Rev.* **1984**, *84*, 577–585.
(10) Jablonski, C. R.; Burrow, T.; Jones, P. G. *J. Organomet. Chem.* **1989**, *370*, 173–185.
(11) Nakazawa, H.; Hiroyuki, N.; Yoshihiko, K.; Yoneda, H. *Organometallics* **1990**, *9*, 1958–1963.
(12) Nakazawa, H.; Morimasa, K.; Kushi, Y.; Yoneda, H. *Organometallics* **1988**, *7*, 458–463.
(13) Nakazawa, H.; Yamaguchi, M.; Kubo, K.; Miyoshi, K. *J. Organomet. Chem.* **1992**, *428*, 145–153.
(14) Valderrama, M.; Scotti, M.; Campos, P.; Werner, H.; Muller, G. *Chem. Ber.* **1990**, *123*, 1005–1011.
(15) Bao, Q. B.; Brill, T. B. *Inorg. Chem.* **1987**, *26*, 3447–3452.
(16) Schleman, E. V.; Brill, T. B. *J. Organomet. Chem.* **1987**, *323*, 103–109.
(17) Sullivan, R. J.; Bao, Q. B.; Landon, S. J.; Rheingold, A. L.; Brill, T. B. *Inorg. Chim. Acta* **1986**, *111*, 19–24.

0276-7333/93/2312-0917$04.00/0

Scheme I

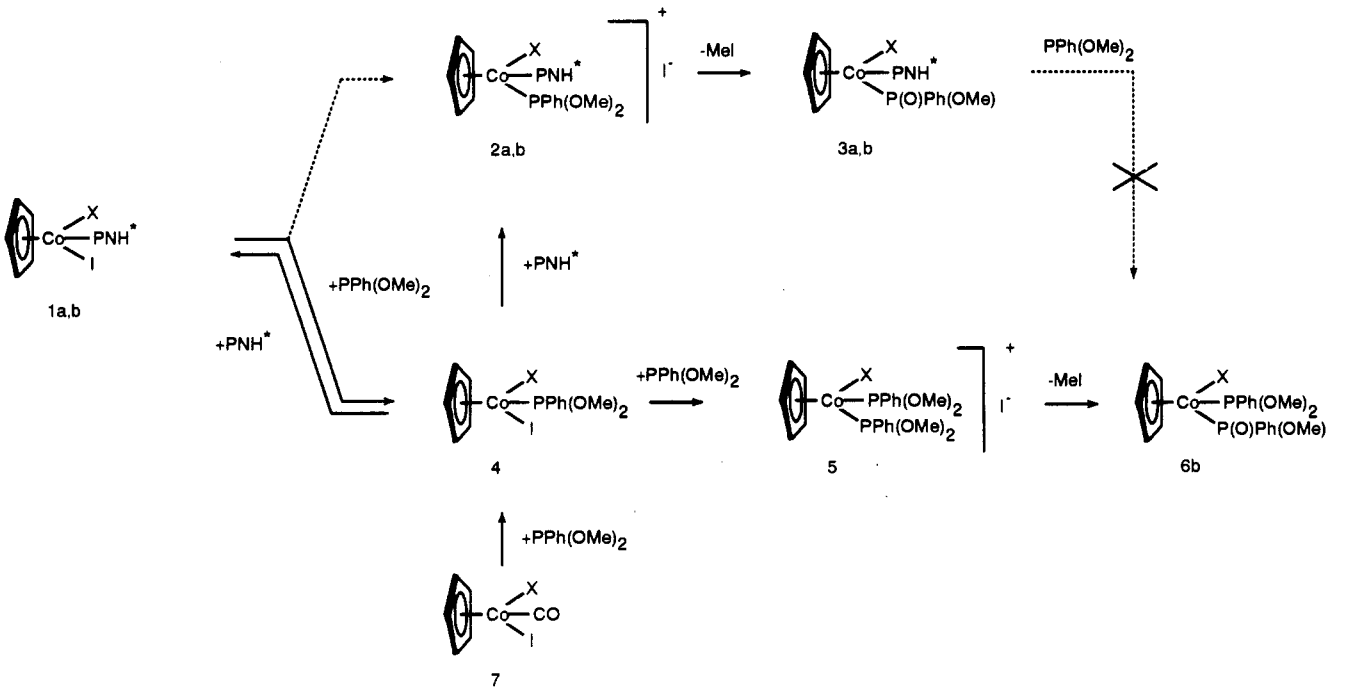

= [**4b**][PNH]/[**1b**][$PPh(OMe)_2$] = 11.8, $CDCl_3$, 30 °C). Phosphinate products **3** and **6** (cf. Scheme I) subsequently form very slowly, presumably by dealkylation of the unobserved cationic phosphonite complexes **2** and **5**, respectively, over a period of several days. We have not analyzed the kinetics of this reaction in detail and therefore cannot at this time unequivocally distinguish whether **2** forms by iodide substitution of **1** and/or **4**. TLC and NMR experiments demonstrated that the phosphinate complex **3b** does not react with excess dimethyl phenylphosphonite in benzene or acetone under the reaction conditions; hence, **6** originates exclusively from direct halide substitution of **4** formed as an intermediate in this sequence. The fact that **3b** is substitution-inert suggests that our previous analysis[10] involving the "tethering" of the aminophosphine by an intramolecular hydrogen bond cannot be correct. Consistent with the proposed facile equilibrium **1** ⇄ **4**, identical phosphinate product distributions result either from treatment of **1** with $PhP(OMe)_2$ or from treatment of **4**, prepared in quantitative yield by carbonyl substitution of **7**, with $PPh_2NHCH(Me)Ph$. The mole ratio of **3**/**6** increased in acetone compared to benzene; hence, it is likely that the direct halide substitution of **1** by $PPh(OMe)_2$ competes more favorably in higher dielectric solvents which support formation of ionic intermediates. The **3**/**6** ratio was maximized by reacting **4** with $PPh_2NHCH(Me)Ph$ in acetone in the presence of **1** to scavenge free phosphonite (cf. Table I). As a further check of the proposed mechanism of Scheme I, **6b** was obtained in good yield by treating **4b** with 1 equiv of $PPh(OMe)_2$ or **7b** with 2 equiv of $PPh(OMe)_2$.

The diastereomeric phosphinate products **3a,b** and **6b** were separated as orange, air-stable solids via a combination of thick-layer radial chromatography and fractional crystallization. The intramolecularly hydrogen bonded (cf. discussion below) aminophosphine derivatives separate as a higher R_f zone with solvent mixtures of moderate polarity. The mixed phosphonite/phosphinate complexes **6b** elute only with very polar solvents. NMR experiments established that the chiral products **3a,b** are configurationally stable at cobalt, phosphorus, and carbon in solution at room temperature for extended periods (weeks). Their structures are fully in accord with analytical data (cf. Table I) and spectroscopic evidence (cf. Tables II and III). The ^1H, ^{13}C, and ^{19}F NMR spectra of the aminophosphine derivatives **3b** are distinct for each diastereomer. For example the ^1H NMR spectrum of the highest R_f diastereomer, $[-2733]_{436}$-**3b**[18] (cf. Table II), shows characteristic Cp (δ 4.90 ppm, s), OMe (δ 3.42 ppm, d, J = 10.9 Hz), C*H (δ 3.63 ppm, m), and C*Me (δ 1.40 ppm, d, J = 6.6 Hz). Both CF_2 groups of the X = C_3F_7 derivatives are diastereotopic, and the ^{19}F NMR spectum typically shows an approximate $ABMNX_3$ pattern. Although a combination of poor signal/noise and peak overlap did not permit definitive assignment of the required aromatic signals for all the derivatives, the aromatic region of the ^{13}C NMR spectrum of $[-2733]_{436}$-**3b** (cf. Table III) clearly reveals three distinct C_{ipso} doublets (δ 143.60, J = 52.0 Hz; δ 138.69, J = 52.7 Hz; δ 133.76, J = 54.2 Hz) and three C_{ortho} doublets (δ 133.75, J = 9.5 Hz; δ 132.41, J = 10.2 Hz; δ 131.21, J = 8.1 Hz) consistent with the presence of a pair of diastereotopic $P(C_6H_5)_2$ groups and a chemically nonequivalent $P-C_6H_5$ group, which are freely rotating about the $P-C_{ipso}$ axis. Additional assignments are presented in Table III.

Solid-State Structure. The solid-state structures of four Co-, P-, and C-chiral methyl phenylphosphinate complexes, **3**, prepared in this study have been determined by X-ray diffraction methods in order to confirm the structure and to establish the absolute configuration. Crystallographic data are presented in Tables IV–IX. Pluto drawings of $[-1325]_{436}$-**3a**, $[+4083]_{436}$-**3a**, $[-2733]_{436}$-**3b**, and $[-1846]_{436}$-**3b** (cf. Table I) are given in Figures 1–4, respectively. All structures demonstrate an unremarkable pseudooctahedral coordination geometry about the cobalt atom with η^5-Cp occupying one face and the remaining interligand bond angles approaching 90°. Relevant bond lengths and angles are given in Table IX.

(18) The notation $[-2733]_{436}$ refers to the specific rotation (deg dL g^{-1} dm^{-1}) at 436 nm and 20 °C.

Table I. Preparative and Physical Data

compd	method[a]	solvent[b]/ temp (°C)/ time (h)	% yield	anal. % C found (calc)	anal. % H found (calc)	anal. % N found (calc)	$[\alpha]_{436}$[d] (deg dL g^{-1} dm^{-1})	abs config	mp (°C)
3a ($C_{33}H_{33}CoF_3NO_2P_2$)	A	B/120/3	30.6	60.23[c]	5.08[c]	2.22[c]	−1325	$R_{Co};R_P;S_C$[e]	154.0–5.5
	A	B/25/48	24.4	(60.65)	(5.09)	(2.14)	+2163	$S_{Co};S_P;S_C$[f]	128.0–35.5
							−3160	$R_{Co};S_P;S_C$[f]	135.0–40.0
							+4083	$S_{Co};R_P;S_C$[e]	182–3[g]
3b ($C_{35}H_{33}CoF_7NO_2P_2$)	A	B/25/2	24.1	55.55[h]	4.54[h]	1.90[h]	−2733	$R_{Co};R_P;S_C$[e]	151–153
	A	A/25/2	38.8	(55.79)	(4.41)	(1.86)	+2607	$S_{Co};S_P;S_C$[f]	186–188
	B	B/25/2	18.7				−1846	$R_{Co};S_P;S_C$[e]	189–190
	B	A/25/2	33.1				+2353	$S_{Co};R_P;S_C$[f]	178–180
	C	A/25/2	14.7[i]						
4a ($C_{21}H_{24}CoF_3O_4P_2$)	D	M/25/1	81	33.92 (34.31)	3.21 (3.29)		rac		146–147
4b ($C_{23}H_{24}CoF_7O_4P_2$)	D	M/25/1	60	32.81 (32.57)	2.85 (2.73)		rac		175–176
6b ($C_{23}H_{24}CoF_7O_4P_2$)	A	B/25/2	38	44.96[j]	4.05[j]		rac		131–138[j]
	A	A/25/2	32.4	(44.68)	(3.91)				149–151[k]
	B	B/25/2	22.7						
	B	A/25/2	30.4						
	C	A/25/2	1.3[i]						

[a] Legend: (A) **1** + $PPh(OMe)_2$; (B) **4** + $PPh_2NHCH(Me)Ph$; (C) **1** + **4** + $PPh_2NHCH(Me)Ph$; (D) **7** + $PPh(OMe)_2$. [b] Legend: B = benzene, A = acetone, M = methylene chloride. [c] $(+2163)_{436}$ diastereomer. [d] Listed in order of decreasing R_f value. [e] Assigned crystallographically. [f] Assigned from CD data. [g] With decomposition. [h] $(+2607)_{436}$ diastereomer. [i] Based on total Co (**1** + **4**). [j] Lower R_f diastereomer. [k] Higher R_f diastereomer.

Table II. ^1H and ^{19}F NMR Spectra[a]

compd	C_6H_5	NH[b]	η^5-C_5H_5	OMe	C*H[c]	C*Me	CF_3/C_3F_7[d]
($R_{Co};R_P;S_C$)-**3a**	7.78 (m)	nf[e]	4.71 (s)	3.68 (d, 10.7)	3.83 (m)	1.46 (d, 6.7)	6.73 (s)
($S_{Co};S_P;S_C$)-**3a**	8.10 (m), 7.82 (m), 7.48 (m), 7.22 (m)	7.03 (dd, 14.4, 10.2)	4.77 (s)	3.68 (d, 10.7)	3.84 (m, 12.7, 10.2, 6.7)	0.99 (d, 6.7)	7.11 (s)
($R_{Co};S_P;S_C$)-**3a**	7.72 (m), 7.43 (m), 7.18 (m), 6.98 (m)	6.08 (dd, 16.8, 9.8)	4.65 (s)	3.56 (d, 11.0)	3.92 (m, 8.8, 9.8, 6.7)	1.45 (d, 6.7)	6.86 (s)
($S_{Co};R_P;S_C$)-**3a**	7.88 (m), 7.70 (m), 7.37 (m), 7.23 (m)	6.23 (dd, 16.5, 10.7)	4.75 (s)	3.62 (d, 11.0)	3.88 (m, 9.6, 10.7, 6.7)	0.93 (d, 6.7)	6.94 (s)
($R_{Co};R_P;S_C$)-**3b**	7.18 (m)	6.76 (dd, 14.1, 8.8)	4.90 (s)	3.42 (d, 10.9)	3.63 (m, 19.5, 8.8, 6.6)	1.40 (d, 6.6)	−66.92, −70.02 (276.7); −113.38, −115.42 (272.2); −78.89 (s)
($S_{Co};S_P;S_C$)-**3b**	8.02 (m), 7.77 (m), 7.20 (m)	6.59 (dd, 13.8, 8.4)	4.93 (s)	3.48 (d, 10.9)	3.85 (m, 11.2, 8.1, 6.7)	1.14 (d, 6.7)	−65.49, −69.53 (276.4); −113.12, −114.98 (275.1); −79.08 (s)
($R_{Co};S_P;S_C$)-**3b**	7.75 (m), 7.62 (m), 7.34 (m), 7.10 (m), 6.98 (m)	6.38 (dd, 16.4, 9.6)	4.71 (s)	3.55 (d, 11.1)	3.79 (m, 10.0, 9.6, 6.7)	1.32 (d, 6.7)	−62.20, −67.61 (271.7); −111.99, −113.22 (277.7); −78.24 (t, 12.4)
($S_{Co};R_P;S_C$)-**3b**	7.90 (m), 7.43 (m), 7.21 (m)	6.47 (dd, 17.8, 10.6)	4.86 (s)	3.52 (d, 11.2)	3.81 (m, 10.5, 10.6, 6.7)	1.01 (d, 6.7)	−65.87, −67.14 (272.9); −112.3, −113.8 (277.5); −78.3 (t, 12.1)
6b (high R_f)	7.88 (m), 7.67 (m), 7.48 (m), 7.34 (m)		5.09 (s)	3.82 (d, 10.9), 3.72 (d, 11.1), 3.40 (d, 11.1)			−64.54, −65.70 (283.3); −113.22, −113.72 (278.3); −79.09 (t, 11.8)
6b (low R_f)	7.73 (m), 7.46 (m), 7.38 (m)		4.98 (s)	3.87 (d, 11.2), 3.81 (d, 11.0), 3.33 (d, 11.2)			−61.93, −67.77 (267.3); −111.77, −114.18 (279.9); −79.13 (t, 10.4)

[a] Measured in $CDCl_3$; δ values relative to internal TMS (^1H) or $CFCl_3$ (^{19}F); J values (in parentheses) given in Hz. [b] $^2J_{HP}$, $^3J_{HH}$. [c] $^3J_{HP}$, $^3J_{(N)HH}$, $^3J_{HH}$. [d] Calculated for $ABMNX_3$: α-CF_2 ($^2J_{AB}$); β-CF_2 ($^2J_{MN}$); δ-CF_3 (^3J). [e] Not found.

Absolute Configurations. Absolute configurations of [−1325]$_{436}$-**3a**, [+4083]$_{436}$-**3a**, [−2733]$_{436}$-**3b**, and [−1846]$_{436}$-**3b** (cf. Table I) were unequivocally assigned as $R_{Co};R_P;S_C$, $S_{Co};R_P;S_C$, $R_{Co};R_P;S_C$, and $R_{Co};S_P;S_C$, respectively, on the basis of crystallographic evidence using modified Cahn–Ingold–Prelog rules[19–21] and the ligand priority sequence η^5-Cp > P(O) > P(N) > perfluoroalkyl for cobalt. The absolute configurations of the remaining two diastereomers for each series were assigned on the basis of chiroptical evidence (circular dichroism (CD) spectroscopy). The CD spectra of [+2163]$_{436}$-**3a** and [−3160]$_{436}$-**3a** are approximate mirror images of those for [−1325]$_{436}$-**3a** and [+4083]$_{436}$-**3a**, respectively (cf. Figure 6), and hence are assigned the opposite hand at cobalt and phosphorus. Ample literature precedent establishes that the morphology of the CD spectrum is dominated by metal-centered electronic transitions,[22] but it is clear that the chiral phosphorus center has a secondary effect. For example, although the

(19) Lecomte, C.; Dusausoy, Y.; Protas, J.; Tirouflet, J.; Dormand, A. *J. Organomet. Chem.* **1974**, *73*, 67–76.
(20) Stanley, K.; Baird, M. C. *J. Am. Chem. Soc.* **1975**, *97*, 6599–6599.
(21) Sloan, T. E. *Top. Stereochem.* **1981**, *12*, 1–36.
(22) Brunner, H. *Angew. Chem. Int. Ed. Engl.* **1971**, *10*, 249–260.

Table III. ^{13}C NMR Spectra[a]

compd	CC_6H_5	PC_6H_5	C_5H_5	OMe	C^*Me	C^*Me
$(R_{Co};R_P;S_C)$-**3a**	i: 146.12	i: 135.71 (d, 32.0)	90.78 (s)	53.92 (d, 11.6)	50.75 (d, 8.7)	27.68 (d, 9.2)
	o, m: 127.29, 125.79	o, m: 132.90 (d, 11.9), 132.15 (d, 9.3), 130.32 (d, 9.6), 127.91 (d, 14.5), 127.74 (d, 11.6), 127.43 (d, 8.5)				
	p: 125.25	p: 130.52 (s), 129.94 (s), 129.44 (s)				
$(S_{Co};S_P;S_C)$-**3a**	i: 146.40	i: 143.54 (d, 55.3), 137.46 (d, 46.3), 134.76 (d, 58.1)	90.74 (s)	53.64 (d, 11.7)	50.81 (d, 9.9)	27.21 (s)
	o, m: 127.29, 125.79	o, m: 132.99 (d, 10.6), 132.40 (d, 10.2), 130.38 (d, 13.3), 127.76 (d, 10.0), 127.57 (d, 10.5), 125.93 (d, 13.8)				
	p: 126.03	p: 130.47 (s), 130.08 (s), 129.47 (s)				
$(R_{Co};S_P;S_C)$-**3a**	i: 145.41	i: 144.63 (d, 53.6), 135.94 (d, 50.1), 135.07 (d, 49.4)	91.26 (s)	53.75 (d, 10.5)	50.47 (d, 10.9)	27.01 (d, 4.5)
	o, m: 127.80, 125.86	o, m: 133.11 (d, 11.0), 132.22 (d, 9.7), 130.46 (d, 10.0)				
		p: 130.29 (s), 130.19 (s), 129.57 (s)				
$(S_{Co};R_P;S_C)$-**3a**	i: 146.00	i: 144.78 (d, 56.1), 136.80 (d, 50.1), 134.83 (d, 58.1)	91.27 (s)	53.75 (d, 11.0)	50.61 (d, 11.7)	26.62 (s)
	o, m: 128.32, 125.75	o, m: 133.17 (d, 11.0), 132.20 (d, 10.1), 127.2 (d, 10.5), 127.58 (d, 10.6)	91.27 (s)	53.75 (d, 11.0)	50.61 (d, 11.7)	26.62 (s)
	p: 126.34	p: 130.61 (s), 130.08 (s), 129.74 (s)				
$(R_{Co};R_P;S_C)$-**3b**	i: 147.50	i: 143.60 (d, 52.0), 138.69 (d, 52.7), 133.76 (d, 54.2)	89.15 (s)	54.05 (d, 11.0)	50.88 (d, 11.0)	26.81 (s)
	o, m: 127.74, 127.54	o, m: 133.75 (d, 9.5), 132.41 (d, 10.3), 131.21 (d, 8.1), 127.21 (d, 10.3)				
	p: 125.97	m: 130.50, 129.59, 129.47				
$(S_{Co};S_P;S_C)$-**3b**	i: 145.43	i: nf[b]	89.22	53.74 (d, 12.1)	50.85 (d, 11.0)	26.81 (s)
	o, m: 127.82, 125.94	o, m: 133.37 (d, 8.6), 123.90 (d, 11.2), 131.08 (d, 9.3), 127.21 (d, 11.6)				
	p: nf	p: 130.18, 129.50, 128.30				
$(R_{Co};S_P;S_C)$-**3b**	i: 145.08	i: 144.20 (d, 52.3), 137.18 (d, 55.3), 134.47 (d, 49.4)	90.37	54.07 (d, 10.6)	50.30 (d, 11.9)	26.40 (s)
	o, m: 127.99, 125.78	o, m: 133.13 (d, 9.8), 132.56 (d, 10.3), 130.80 (d, 9.7), 127.71 (d, 11.5)				
	p: 126.22	p: 130.26, 129.99, 129.57				
$(S_{Co};R_P;S_C)$-**3b**	i: 145.91	i: 144.70 (d, 52.9)	90.02	54.08 (d, 10.4)	50.62 (d, 10.9)	26.89 (s)
	o, m: 127.79, 126.10	o, m: 133.13 (d, 9.8), 132.56 (d, 12.8), 131.10 (d, 9.7), 128.06 (d, 9.5), 127.45 (d, 10.2)				
	p: 126.22	p: 130.37, 129.89, 129.82				
6b (high R_f)		i: 143.73 (d, 58.2), 137.127 (d, 58.1)	89.96	55.44 (d, 11.5)		
		o, m: 131.25 (d, 10.6), 130.93 (d, 11.2), 128.05 (d, 10.4), 127.15 (d, 11.1)		54.26 (d, 10.4)		
		p: 131.00 (s), 129.21 (s)		50.69 (d, 10.9)		
6b (low R_f)		i: 144.48 (d, 58.3), 136.57 (d, 58.7)	90.28	55.00 (d, 11.1)		
		o, m: 131.25 (d, 10.6), 130.58 (d, 10.0), 127.83 (d, 12.9), 127.67 (d, 11.5)		54.74 (d, 10.4)		
		p: 130.93 (s), 129.29 (s)		49.96 (d, 12.1)		

[a] Measured in $CDCl_3$; δ values relative to solvent $CDCl_3$ 77.0 ppm; J values (in parentheses) given in Hz. [b] nf = not found.

P-epimeric diastereomeric complexes $[-1325]_{436}$-$(R_{Co};R_P;S_C)$-**3a** and $[-3160]_{436}$-$(R_{Co};S_P;S_C)$-**3a** have similar positive Cotton effects in the region of 360 and 455–470 nm and negative Cotton effects in the region of 325 and 380–415 nm, there are characteristic intensity and energy differences ascribable to the stereogenic phosphorus center (cf. Figure 6). A similar rationale applies for the assignment of absolute configuration in the **3b** series. Interestingly the relative chromatographic R_f values found for both series **3a** and **3b** are reliable indicators of absolute configuration. The absolute configurations $R_{Co};R_P;S_C$, $S_{Co};S_P;S_C$, $R_{Co};S_P;S_C$, and $S_{Co};R_P;S_C$ in order of decreasing R_f values determined in this study follow the same pattern found previously[3] for the X = I series.

Conformational Analysis. The solid-state structures of Figures 1–4 show the presence of a strong P=O···H—N intramolecular hydrogen bond in the aminophosphine/methyl phenylphosphinate products, and significantly, all four structures crystallize in the same "chaise lounge" Co—P=O···H—N—P six-membered-ring conformation (Figure 5) observed previously for related iodo[3] and perfluoroalkyl derivatives.[4] We conclude that the conformational preferences for the aminophosphine/phosphinate complexes are of a general nature and are not strongly influenced by crystal-packing forces. The N—O distances of 2.806, 2.711, 2.716, and 2.815 Å for $[-1325]_{436}$-**3a**, $[+4083]_{436}$-**3a**, $[-2733]_{436}$-**3b**, and $[-1846]_{436}$-**3b**, respectively, are significantly shorter than the value of 3.05(6) Å considered diagnostic[23] for O···H—N bonding. As found for other complexes of the general formula $(\eta^5\text{-Cp})$Co(X)(PNH*)(P(O)R(OR),[4,24] the η^5-Cp group is pseudoequatorial and the perfluoroalkyl group occupies a pseudoaxial position (cf. Figure 5). In this conformation

(23) Whuler, A.; Brouty, C.; Spinat, P. *Acta Crystallogr.* **1980**, *B36*, 1267–1269.
(24) Brunner, H.; Ernst, J.; Wischert, T.; Thewalt, U. *J. Organomet. Chem.* **1987**, *328*, 331–339.

Table IV. Crystallographic Data

	$[-1325]_{436}$-**3a**	$[+4083)_{436}$-**3a**	$[-2733]_{436}$-**3b**	$[-1846]_{436}$-**3b**
		(a) Crystal Parameters		
formula	$CoC_{33}H_{33}NO_2P_2F_3$	$CoC_{33}H_{33}NO_2P_2F_3$	$CoC_{35}H_{33}NO_2P_2F_7$	$CoC_{35}H_{33}NO_2P_2F_7{\cdot}CH_2Cl_2$
fw	653.51	653.51	753.52	838.45
cryst syst	orthothrombic	trigonal	orthorhombic	orthorhombic
space group	$P2_12_12_1$ (No. 19)	$P3_1$ (No. 144)	$P2_12_12_1$ (No. 19)	$P2_12_12_1$ (No. 19)
a, Å	8.7863(12)[a]	14.9469(14)[b]	12.4590(14)[c]	15.929(3)[d]
b, Å	17.2439(19)[a]		16.1554(22)[c]	17.670(2)[d]
c, Å	21.3634(19)[a]	12.2911(8)[b]	17.6204(14)[c]	13.549(2)[d]
V, Å^3	3236.8(6)	2378.1(3)	3546.6(7)	3813.6(9)
Z	4	3	4	4
cryst dimens (mm)	0.25 × 0.20 × 0.05	0.07 × 0.07 × 0.30	0.35 × 0.30 × 0.30	0.35 × 0.35 × 0.20
cryst color	orange	orange	orange	orange
D_{calc} (g cm^{-3})	1.341	1.369	1.411	1.460
F_{000}	1351.8	1013.85	1543.79	1712
μ (cm^{-1})	6.7	58.2	6.4	7.37
temp (K)	297	297	297	299
		(b) Data Collection		
diffractometer	Nonius CAD 4	Nonius CAD 4	Nonius CAD 4	Rigaku AFC6S
monochromator	graphite	graphite	graphite	graphite
radiation	Mo Kα (λ = 0.709 30 Å)	Cu Kα (λ = 1.540 56 Å)	Mo Kα (λ = 0.709 30 Å)	Mo Kα (λ = 0.710 69 Å)
2θ(max) (deg)	44.9	99.8	44.7	50.0
data collected (hkl)	0–8, −17 to +18.0–22	−12 to +12, 0–14, 0–12	−11 to +12, −15 to +16, −17 to +18	
abs cor	no	no	no	yes[e]
no. of rflns collected	8146	1609	2569	7532
no. of unique rflns	4154	1609	2569	3765
no. of rflns with $F_o \geq n\sigma(F_o)$	2588 (n = 2.5)	1057 (n = 2.5)	2096 (n = 2.5)	2113 (n = 3.0)
		(c) Refinement		
R_F (%)	6.6	6.8	6.5	6.3
R_{wF} (%)	2.7	4.0	5.1	4.7
Δ/σ(max)	0.120	0.357	0.094	0.18
$\Delta(\rho)$(max/min) (e Å^{-3})	0.400/−0.370	0.350/−0.300	0.460/−0.480	0.65/−0.68
GOF	2.16	3.52	3.96	2.49

[a] Cell dimensions obtained from 23 reflections with 26.00° ≤ 2θ ≥ 30.00°. [b] Cell dimensions obtained from 27 reflections with 60.00° ≤ 2θ ≥ 65.00°. [c] Cell dimensions obtained from 31 reflections with 36.00° ≤ 2θ ≥ 45.00°. [d] Cell dimensions obtained from 25 reflections with 27.80° ≤ 2θ ≥ 32.72°. [e] Empirical absorption corrections calculated using the program DIFABS.[32]

the η^5-Cp ring is gauche with respect to the diastereotopic PPh_2 rings as well as to both phosphinate substituents.

The solution conformation of the methyl phenylphosphinate products was investigated using ^{1}H nuclear Overhauser difference effect spectroscopy (NOED).[25] The results (cf. Figure 7) are consistent with significant population of the solid-state "chaise lounge" conformations presented for (S_{Co};S_P)-**3a,b** and (R_{Co};S_P)-**3a,b** in Figure 5 and redrawn viewed along the Cp–Co bond axis in Figure 8. Partial saturation of the cyclopentadienyl resonance of (R_{Co};R_P;S_C)-**3a,b** or (S_{Co};S_P;S_C)-**3a,b**, obtained as the major products in the Arbuzov chemistry, gave reproducible enhancements (ca. +5%, Figure 7a) for *three* o-P*Ph* multiplets, suggesting significant population of a conformation with an equatorial Cp and hence three cyclopentadienyl/P-phenyl (rings A–C, cf. Figure 7c) gauche interactions. Similarly, partial saturation of the P–O*Me* signal enhanced (ca. 3%) multiplets assigned to *two* o-P*Ph* multiplets of rings A and C (cf. Figure 7c). The ortho Ph multiplet of ring A was definitively assigned on the basis of a positive NOE enhancement from both the C**H* and C**Me* signals. The aromatic region of the NOED spectra obtained for the minor diastereomers (R_{Co};S_P;S_C)-**3a,b** or (S_{Co};R_P;S_C)-**3a,b** again shows medium-intensity NOE enhancements to the three o-P*Ph* multiplets of rings A–C (cf. Figure 7a). Since the P–O*Me* group is now pseudoaxial as shown in Figure 8, there is only one gauche PPh group (C) and only one medium-intensity NOE enhancement is observed (Figure 7c) in the appropriate NOED experiment.

(25) Neuhaus, D.; Williamson, M. P. *The Nuclear Overhauser Effect in Structural and Conformational Analysis*; VCH: New York, 1989.

Co*→P Chiral Induction. Kinetic product ratios for **1a,b** → **3a,b** were measured at low percent conversion by NMR integration. Table X shows that Co*→P optical induction is low, in the range of 25–55% de. Comparison with our earlier studies[3] of the iodo series **3b** (X = I) shows that optical inductions decrease with the substitution of CF_3 or C_3F_7 for iodide. In general optical yields for the formation of a stereogenic P center in the reaction **1** → **3** of Scheme I increase with increasing steric requirements along the series X = CF_3 (25–30% de) < C_3F_7 (45–55% de) < I (75–80% de). Observation of Table X identifies the metal atom as the source of chirality, since the stereochemistry created at phosphorus responds cleanly to the configuration at cobalt. In each case examined the major diastereomer proved to have the *same* absolute configuration at cobalt and phosphorus and we note that this is the same *relative* stereochemistry obtained previously.[3]

We interpret the chiral inductions obtained for the transformation **1** → **3** on the assumption of the mechanism shown in Scheme I and a "chaise lounge" solution conformation with pseudoequatorial η^5-Cp as shown in Figures 5 and 8.[3] Chiral Co*→P induction occurs in the cationic dimethyl phenylphosphonite **2** formed via direct halide substitution or via the sequence **1** → **4** → **2**. The stereochemistry of S_N2 nucleophilic attack at carbon on the diastereotopic OMe phosphonite groups by iodide evolves under the influence of the chiral Co atom. Assuming that the phosphoryl P=O bond and intramolecular P=O···H—N are sufficiently well developed, the transition state for formation of (S_{Co};S_P)-**3** and (R_{Co};S_P)-**3** will resemble the product conformations of Figures 5 and

Table V. Fractional Atomic Coordinates and Isotropic Thermal Parameters for $[-1325]_{436}$-(R_{Co};R_P;S_C)-3a

atom	x	y	z	B_{iso}[a] (Å^2)
Co	0.72306(21)	0.99483(12)	0.81790(7)	3.48(10)
P1	0.6830(4)	0.99583(22)	0.71539(11)	3.44(19)
P2	0.9656(5)	0.95724(21)	0.81308(17)	3.99(22)
F1	0.6611(9)	1.1504(4)	0.8069(3)	6.7(5)
F2	0.8882(9)	1.1291(4)	0.7797(3)	5.9(5)
F3	0.8291(10)	1.1275(4)	0.8767(3)	6.5(5)
O1	1.0650(8)	0.9881(5)	0.7620(3)	4.9(5)
O2	0.9607(10)	0.8637(4)	0.8136(4)	5.8(6)
N	0.8364(11)	1.0200(5)	0.6748(3)	3.6(5)
C1	0.6658(19)	0.8974(7)	0.8745(6)	6.1(4)
C2	0.5498(17)	0.9141(8)	0.8345(6)	6.7(4)
C3	0.4880(15)	0.9856(9)	0.8444(6)	6.3(4)
C4	0.5761(15)	1.0198(6)	0.8931(5)	4.6(3)
C5	0.6911(16)	0.9670(6)	0.9107(4)	4.6(3)
C6	0.7783(18)	1.1004(7)	0.8180(7)	4.9(3)
C7	0.8490(13)	1.0076(7)	0.6055(4)	3.2(3)
C8	0.9536(15)	1.0677(6)	0.5813(4)	4.8(3)
C9	1.1016(17)	0.8232(7)	0.7984(6)	7.8(5)
C11*[b]	0.5393(8)	1.0657(4)	0.6919(3)	3.28(13)
C12*	0.5866(7)	1.1352(5)	0.6647(3)	5.21(13)
C13*	0.4802(10)	1.1927(4)	0.6507(3)	5.67(13)
C14*	0.3265(9)	1.1807(4)	0.6639(3)	5.46(13)
C15*	0.2792(6)	1.1112(5)	0.6911(3)	4.71(13)
C16*	0.3856(9)	1.0537(3)	0.70508(23)	4.13(13)
C21*	0.6145(8)	0.9043(3)	0.6834(3)	3.14(13)
C22*	0.5073(9)	0.9021(3)	0.6352(4)	3.89(13)
C23*	0.4732(8)	0.8319(5)	0.6059(3)	4.87(13)
C24*	0.5464(9)	0.7640(3)	0.6247(3)	4.27(13)
C25*	0.6535(8)	0.7663(3)	0.6729(3)	4.86(13)
C26*	0.6876(6)	0.8364(5)	0.70218(22)	4.22(13)
C31*	0.8984(8)	0.9267(3)	0.5890(3)	3.13(13)
C32*	0.8245(7)	0.8885(4)	0.5401(3)	3.12(13)
C33*	0.8693(9)	0.8138(4)	0.5231(3)	4.44(13)
C34*	0.9879(9)	0.7773(3)	0.5550(3)	4.92(13)
C35*	1.0617(6)	0.8155(4)	0.6039(3)	3.88(13)
C36*	1.0170(8)	0.8902(4)	0.62093(24)	3.25(13)
C41*	1.0626(7)	0.9809(5)	0.8868(3)	5.61(17)
C42*	1.0684(9)	0.9285(4)	0.9365(4)	6.61(17)
C43*	1.1434(11)	0.9486(4)	0.9917(3)	7.26(17)
C44*	1.2124(9)	1.0211(5)	0.9972(3)	6.77(17)
C45*	1.2066(8)	1.0735(3)	0.9475(4)	7.52(17)
C46*	1.1316(10)	1.0534(4)	0.8923(3)	5.50(17)

[a] B_{iso} is the mean of the principal axes of the thermal ellipsoid. [b] Refined as rigid phenyl groups.

Table VI. Fractional Atomic Coordinates and Isotropic Thermal Parameters for $[+4083]_{436}$-(S_{Co};R_P;S_C)-3a

atom	x	y	z	B_{iso}[a] (Å^2)
Co	0.62398(21)	0.76454(21)	0.13137	5.02(22)
P1	0.7896(4)	0.8408(4)	0.1716(4)	6.9(4)
P2	0.5773(4)	0.6178(4)	0.2174(3)	4.6(4)
F1	0.6302(8)	0.8141(7)	0.3538(6)	8.5(9)
F2	0.4970(8)	0.7932(8)	0.2715(7)	9.1(9)
F3	0.6444(8)	0.9330(7)	0.2483(8)	9.8(10)
O1	0.8188(9)	0.8253(9)	0.2838(8)	9.5(10)
O2	0.8311(9)	0.9578(8)	0.1449(9)	8.5(10)
N	0.6557(9)	0.6311(9)	0.3170(9)	5.0(10)
C1	0.5341(12)	0.6799(12)	–0.0054(12)	5.7(5)
C2	0.4878(12)	0.7337(12)	0.0396(12)	6.0(5)
C3	0.5654(13)	0.8374(13)	0.0356(13)	7.6(6)
C4	0.6549(12)	0.8537(12)	–0.0088(13)	6.4(5)
C5	0.6359(12)	0.7540(12)	–0.0359(12)	5.5(5)
C6	0.6026(12)	0.8346(12)	0.2601(13)	6.4(5)
C7	0.9236(20)	1.0382(19)	0.1959(22)	18.5(10)
C8	0.6435(12)	0.5421(12)	0.3764(13)	6.8(5)
C9	0.7429(15)	0.5263(14)	0.3619(13)	9.3(6)
C11*[b]	0.8677(9)	0.8126(9)	0.0778(11)	10.2(3)
C12*	0.9100(12)	0.7531(9)	0.1135(8)	12.1(3)
C13*	0.9705(11)	0.7321(11)	0.0432(12)	13.1(3)
C14*	0.9887(10)	0.7706(9)	–0.0628(12)	13.7(3)
C15*	0.9464(11)	0.8302(7)	–0.0985(8)	14.9(3)
C16*	0.8859(10)	0.8512(9)	–0.0281(11)	11.3(3)
C21*	0.5715(9)	0.5137(7)	0.1313(7)	6.25(22)
C22*	0.4899(8)	0.4120(8)	0.1366(8)	6.85(22)
C23*	0.4922(8)	0.3355(6)	0.0736(10)	7.49(22)
C24*	0.5761(9)	0.3607(7)	0.0053(8)	8.71(22)
C25*	0.6576(6)	0.4623(9)	0.0000(7)	8.96(22)
C26*	0.6553(7)	0.5388(6)	0.0629(7)	5.68(22)
C31*	0.4479(7)	0.5612(7)	0.2735(10)	5.19(20)
C32*	0.4403(7)	0.5775(8)	0.3841(9)	5.54(20)
C33*	0.3439(9)	0.5458(10)	0.4306(6)	5.46(20)
C34*	0.2550(6)	0.4978(8)	0.3665(10)	7.19(20)
C35*	0.2626(7)	0.4815(6)	0.2560(9)	5.78(20)
C36*	0.3590(10)	0.5132(7)	0.2095(6)	6.71(20)
C41*	0.6389(8)	0.5565(11)	0.5028(7)	5.73(25)
C42*	0.5676(8)	0.4714(7)	0.5631(11)	7.11(25)
C43*	0.5587(8)	0.4809(8)	0.6750(11)	10.37(25)
C44*	0.6209(9)	0.5753(11)	0.7264(7)	8.39(25)
C45*	0.6922(7)	0.6604(7)	0.6661(11)	10.52(25)
C46*	0.7011(7)	0.6509(8)	0.5543(11)	8.08(25)

[a] B_{iso} is the mean of the principal axes of the thermal ellipsoid. [b] Refined as rigid phenyl groups.

8. Relatively unobstructed nucleophilic attack on the pro-*S* OMe forms an S_P chiral center from S_{Co}, avoiding the 1,3-diaxial steric interaction present in the transition state leading to (R_{Co};S_P)-**3**. Solid-state and solution studies require a pseudoaxial position for X regardless of its steric requirements, and this is confirmed by the relative stereochemistry of the major diastereomers observed. A preference for pseudoequatorial X would lead to a strong 1,3-diaxial interaction for the transition state leading to (S_{Co};S_P)-**3** and the major product would be expected to have the opposite hand, (R_{Co};S_P)-**3**. Increasing steric bulk of the pseudoaxial X substituent may exert a "buttressing" effect, which contributes to the difference in energies of the diastereomeric transition states related to Figures 5 and 8.

Summary

Chiral piano-stool Co(III) halides (η^5-Cp)Co(PPh_2-NHCH(Me)Ph)(X)(I) (X = CF_3, C_3F_7) react with dimethyl phenylphosphonite in an Arbuzov-like dealkylation to afford methyl phenylphosphinate products (η^5-Cp)Co-(PPh_2NHCH(Me)Ph)(X)(P(O)(OMe)Ph) (**3**) and (η^5-Cp)Co($P(OMe)_2$Ph)(X)(P(O)(OMe)Ph) (**6**), which are chiral at cobalt and phosphoryl phosphorus. The absolute configurations of eight configurationally stable methyl phenylphosphinate products have been determined using a combination of X-ray and chiroptical methods. The reaction proceeds via initial substitution of the neutral aminophosphine ligand to give (η^5-Cp)Co($P(OMe)_2$Ph)-(X)(I) **4**, which has been characterized. Displacement of iodide by either PPh_2NHCH(Me)Ph or $P(OMe)_2$Ph affords an unobserved cationic intermediate which dealkylates to give the isolated methyl phenylphosphinate products. The Arbuzov dealkylations show moderate to low diastereoselectivity which increases along the series X = CF_3 < C_3F_7 < I.

Experimental Section

Reagents and Methods. All manipulations were performed under a nitrogen atmosphere using standard Schlenk techniques. Nitrogen gas was purified by passing through a series of columns containing granular phosphorus pentoxide, 3A molecular sieves, and BASF DEOX catalyst (100 °C). Toluene, benzene, and ether were distilled under a nitrogen atmosphere from blue solutions of sodium benzophenone ketyl. Methylene chloride was freshly distilled from P_4O_{10}. Acetone was distilled from activated 3A molecular sieves. The progress of reactions was monitored by analytical thin-layer chromatography (precoated TLC plates, silica gel F-254, Merck). NMR spectra were recorded on a General

Table VII. Fractional Atomic Coordinates and Isotropic Thermal Parameters for $[-2733]_{436}$-(R_{Co};R_P;S_C)-3b

atom	x	y	z	B_{iso}[a] (Å^2)
Co	0.01265(14)	0.47666(9)	0.79436(9)	3.18(8)
P1	0.1692(3)	0.52625(20)	0.75536(19)	2.97(15)
P2	-0.0539(3)	0.60334(20)	0.81457(21)	3.31(18)
F1	0.0294(6)	0.4368(4)	0.6389(4)	4.7(4)
F2	-0.0612(5)	0.5484(4)	0.6572(4)	4.6(4)
F3	-0.2292(6)	0.4483(4)	0.7174(5)	5.7(4)
F4	-0.1343(7)	0.3426(4)	0.6825(5)	6.5(5)
F5	-0.2809(8)	0.3841(6)	0.5847(6)	10.5(7)
F6	-0.1276(8)	0.4101(9)	0.5400(6)	12.3(9)
F7	-0.2292(10)	0.5056(6)	0.5758(6)	11.6(8)
O1	-0.0082(7)	0.6744(4)	0.7707(4)	3.9(4)
O2	-0.0388(7)	0.6193(5)	0.9049(5)	4.3(5)
N	0.1592(7)	0.6059(5)	0.6945(5)	3.24(21)
C1	0.0099(11)	0.3485(7)	0.8145(7)	4.2(3)
C2	0.0992(11)	0.3853(9)	0.8539(8)	5.0(4)
C3	0.0556(11)	0.4449(9)	0.9042(8)	4.5(3)
C4	-0.0556(11)	0.4423(8)	0.9016(8)	3.7(3)
C5	-0.0842(11)	0.3845(9)	0.8458(8)	3.9(3)
C6	-0.0426(10)	0.4733(8)	0.6903(7)	3.5(3)
C7	-0.1483(12)	0.4244(10)	0.6697(9)	5.0(4)
C8	-0.1950(17)	0.4319(13)	0.5890(12)	7.0(5)
C9	-0.0547(10)	0.7024(8)	0.9336(7)	4.3(3)
C10	0.2069(10)	0.6231(7)	0.6206(7)	3.7(3)
C11	0.1216(11)	0.6559(8)	0.5673(7)	4.5(3)
C21	-0.2005(10)	0.6111(8)	0.8038(8)	4.0(3)
C22	-0.2399(12)	0.6449(8)	0.7395(8)	5.1(4)
C23	-0.3529(14)	0.6530(11)	0.7284(9)	7.6(5)
C24	-0.4132(13)	0.6245(11)	0.7828(10)	7.5(5)
C25	-0.3834(15)	0.5928(11)	0.8459(10)	8.0(5)
C26	-0.2678(13)	0.5818(9)	0.8589(9)	6.1(4)
C31	0.2668(10)	0.4580(8)	0.7099(8)	3.8(3)
C32	0.3694(10)	0.4883(8)	0.6984(8)	4.7(3)
C33	0.4478(11)	0.4394(9)	0.6643(8)	5.6(4)
C34	0.4244(12)	0.3606(9)	0.6402(9)	6.0(4)
C35	0.3250(12)	0.3309(8)	0.6528(8)	4.9(3)
C36	0.2442(10)	0.3774(8)	0.6875(7)	3.8(3)
C41	0.2452(10)	0.5608(7)	0.8372(7)	3.4(3)
C42	0.2217(10)	0.6383(8)	0.8697(7)	3.7(3)
C43	0.2708(12)	0.6630(8)	0.9381(8)	5.4(4)
C44	0.3406(11)	0.6121(9)	0.9752(8)	5.4(4)
C45	0.3646(10)	0.5344(9)	0.9445(7)	4.8(3)
C46	0.3157(10)	0.5097(7)	0.8765(7)	4.0(3)
C51	0.2972(12)	0.6828(9)	0.6269(9)	5.1(4)
C52	0.3138(10)	0.7375(7)	0.6857(8)	3.9(3)
C53	0.3950(13)	0.7999(10)	0.6851(10)	7.0(5)
C54	0.4609(17)	0.7996(12)	0.6255(12)	10.4(6)
C55	0.4573(19)	0.7441(14)	0.5706(13)	13.6(8)
C56	0.3773(16)	0.6825(11)	0.5706(11)	8.9(5)

[a] B_{iso} is the mean of the principal axes of the thermal ellipsoid.

Table VIII. Fractional Atomic Coordinates and Isotropic Thermal Parameters for $[-1846]_{436}$-(R_{Co};S_P;S_C)-3b

atom	x	y	z	B(eq) (Å^2)
Co	0.5871(1)	0.3861(1)	0.0503(1)	2.98(7)
Cl1	0.1713(4)	0.3384(5)	0.4481(5)	18.7(6)
Cl2	0.0688(6)	0.2805(5)	0.5829(9)	31(1)
P1	0.5831(2)	0.4796(2)	-0.0607(3)	3.1(2)
P2	0.4640(2)	0.3338(2)	0.0057(3)	3.0(2)
F1	0.4513(4)	0.4738(4)	0.1281(5)	4.4(4)
F2	0.5729(5)	0.5270(4)	0.1477(5)	4.5(4)
F3	0.5087(6)	0.3645(5)	0.2745(6)	6.3(5)
F4	0.6106(6)	0.4425(6)	0.2991(7)	8.6(7)
F5	0.4899(7)	0.4733(8)	0.4193(8)	11.6(9)
F6	0.485(1)	0.5591(6)	0.309(1)	14(1)
F7	0.3958(6)	0.4695(6)	0.3122(8)	9.0(7)
O1	0.5011(4)	0.5208(4)	-0.0727(6)	3.0(4)
O2	0.6576(5)	0.5380(5)	-0.0293(6)	4.0(5)
N1	0.3984(5)	0.3908(5)	-0.0490(8)	3.4(5)
C1	0.6980(9)	0.376(1)	0.133(1)	5.2(9)
C2	0.7174(7)	0.3830(9)	0.035(1)	5.2(9)
C3	0.6820(8)	0.3186(8)	-0.015(1)	4.9(9)
C4	0.6421(8)	0.2762(7)	0.056(1)	4.5(8)
C5	0.6502(9)	0.3090(8)	0.148(1)	4.3(8)
C6	0.5351(8)	0.4560(8)	0.149(1)	3.9(7)
C7	0.535(1)	0.437(1)	0.260(1)	6(1)
C8	0.477(1)	0.489(1)	0.324(1)	7(1)
C9	0.655(1)	0.6158(8)	-0.064(1)	8(1)
C10	0.3227(8)	0.3675(7)	-0.103(1)	4.8(8)
C11	0.2445(7)	0.4067(9)	-0.064(1)	7(1)
C57	0.116(1)	0.3575(9)	0.572(2)	13(2)
C21*[a]	0.6168(5)	0.4525(4)	-0.1861(5)	2.9(3)
C22*	0.5547(4)	0.4323(4)	-0.2539(6)	4.0(3)
C23*	0.5769(5)	0.4117(4)	-0.3498(6)	5.0(3)
C24*	0.6611(6)	0.4112(4)	-0.3779(5)	5.5(4)
C25*	0.7232(4)	0.4314(4)	-0.3102(6)	5.5(4)
C26*	0.7010(4)	0.4520(4)	-0.2143(6)	3.8(3)
C31*	0.4070(5)	0.2960(5)	0.1102(5)	3.4(3)
C32*	0.4341(4)	0.2310(5)	0.1591(7)	4.8(3)
C33*	0.3912(6)	0.2054(4)	0.2424(6)	6.6(4)
C34*	0.3212(6)	0.2448(5)	0.2768(5)	6.2(4)
C35*	0.2941(4)	0.3098(5)	0.2279(7)	6.3(4)
C36*	0.3370(5)	0.3354(4)	0.1446(6)	4.7(3)
C41*	0.4748(5)	0.2532(4)	-0.0765(5)	3.3(3)
C42*	0.4295(4)	0.1864(5)	-0.0636(5)	4.4(3)
C43*	0.4372(5)	0.1277(4)	-0.1318(7)	5.6(4)
C44*	0.4904(5)	0.1358(4)	-0.2130(6)	5.7(4)
C45*	0.5358(4)	0.2026(5)	-0.2259(5)	4.5(3)
C46*	0.5280(4)	0.2613(4)	-0.1577(6)	4.2(3)
C51*	0.3302(5)	0.3782(7)	-0.2142(5)	4.4(3)
C52*	0.3386(6)	0.3154(4)	-0.2758(9)	7.8(5)
C53*	0.3496(6)	0.3253(5)	-0.3771(8)	9.1(5)
C54*	0.3524(5)	0.3981(7)	-0.4168(5)	8.4(5)
C55*	0.3441(5)	0.4609(5)	-0.3553(9)	8.6(5)
C56*	0.3330(5)	0.4510(5)	-0.2540(8)	6.4(4)

[a] Refined as rigid groups.

Electric GN300-NB spectrometer. Optical rotation measurements were determined in toluene (ca. 1 mg/mL) in a 1 cm pathlength cell using a Perkin-Elmer Model 141 polarimeter. CD spectra were determined in toluene (ca. 1 mg/mL) on a Jasco J 40 A apparatus using a 0.1 cm pathlength cell. Melting points were determined in sealed capillaries and are uncorrected. Elemental analyses were performed by Guelph Chemical Laboratories, Inc., Guelph, Ontario, Canada, or Canadian Microanalytical Service, Inc., Delta, BC, Canada. Chromatographic purifications were carried out using a Chromatotron (Harrison Associates) with 1–2 mm thick silica gel$_{60}$PF$_{254}$ (Merck) adsorbant. The compounds (*S*)-(-)-PPh$_2$NHC*H(Me)Ph[26] (PNH*), (η^5-Cp)CoI(CO)X,[27] and (η^5-Cp)CoI(PPh$_2$NHCH(Me)Ph)X (**1a,b**)[4,28] were prepared using the established procedures. Commercial samples of dimethyl phenylphosphonite (Aldrich), CF_3I (Aldrich), and C_3F_7I (Aldrich) were used as received.

Proton NOED spectra[25] were determined under steady-state conditions on a GE300-NB instrument. Data was collected on ca. 5 mg degassed samples in 0.6 mL of $CDCl_3$ or acetone-d_6 using interleaved experiments of 16 transients cycled 32 times through the list of decoupling frequencies. In each experiment the decoupler was gated in continuous wave (CW) mode for 3–6 s with sufficient attenuation to give an approximate 70–90% reduction in intensity of the irradiated peak. A 60-s delay preceeded each frequency change. A set of four equilibrating scans was employed to equilibrate the spins prior to data acquisition. No relaxation delay was applied between successive scans of a given frequency. Difference spectra were obtained on zero-filled 32K data tables which had been digitally filtered with a 0.1-Hz exponential line-broadening function. Quantitative data were obtained by integration.

Crystal Structure Determinations. Crystallographic data were collected at room temperature on an Enraf-Nonius CAD4 ($[-1325]_{436}$-(R_{Co};R_P;S_C)-**3a**, $[+4083]_{436}$-(S_{Co};R_P;S_C)-**3a**, and $[-2733]_{436}$-(R_{Co};R_P;S_C)-**3b**) under the control of the NRCCAD program[29] or a Rigaku AFC6s ($[-1846]_{436}$-(R_{Co};S_P;S_C)-**3b**·CH_2Cl_2) automated diffractometer using graphite-monochromated

(26) Brunner, H.; Doppelberger, J. *Chem. Ber.* **1978**, *111*, 673–691.
(27) King, R. B.; Treichel, P. M.; Stone, F. G. A. *J. Am. Chem. Soc.* **1961**, *83*, 3593.
(28) Brunner, H.; Doppelberger, J.; Dreischl, P.; Moellenberg, T. *J. Organomet. Chem.* **1977**, *139*, 223–233.

Table IX. Selected Bond Distances (Å) and Angles (deg)

	(R_{Co};R_P;S_C)-**3a**	(S_{Co};R_P;S_C)-**3a**	(R_{Co};R_P;S_C)-**3b**	(R_{Co};S_P;S_C)-**3b**
Co–P(N)	2.218(3)	2.210(5)	2.218(4)	2.250(4)
Co–P(O)	2.230(5)	2.202(6)	2.237(4)	2.235(4)
Co–C(X)	1.884(12)	2.009(16)	1.959(12)	2.00(1)
Co–C1	2.131(12)	2.128(15)	2.101(11)	2.10(1)
Co–C2	2.092(14)	2.165(16)	2.107(15)	2.09(1)
Co–C3	2.148(13)	2.072(16)	2.120(12)	2.12(1)
Co–C4	2.106(11)	2.083(16)	2.072(14)	2.13(1)
Co–C5	2.059(10)	2.076(15)	2.146(14)	2.15(1)
P=O	1.496(9)	1.499(11)	1.497(8)	1.505(8)
P–OCH_3	1.613(8)	1.570(12)	1.623(9)	1.628(8)
P–N	1.656(10)	1.638(12)	1.680(10)	1.63(1)
N–C	1.499(11)	1.447(19)	1.458(10)	1.47(2)
C(X)–Co–P(N)	92.0(5)			94.1(4)
C(X)–Co–P(O)	92.0(5)		92.6(4)	88.9(4)
P(N)–Co–P(O)	96.22(15)	97.0(20)	92.57(14)	95.6(1)
O=P–O	112.1(5)	112.4(7)	109.9(4)	110.7(4)
O=P–Co	119.2(4)	117.8(5)	118.6(4)	117.1(3)
O–P–Co	105.4(4)	104.2(5)	105.0(3)	105.8(3)
P–O–C	117.0(7)	121.1(13)	118.3(7)	119.9(8)
P–N–C	122.7(7)	120.8(10)	133.3(8)	125.4(8)

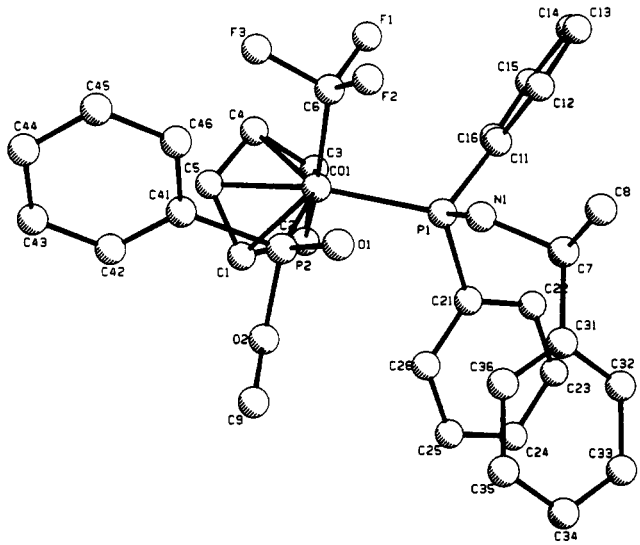

Figure 1. Structure of $[-1325]_{436}$-**3a**.

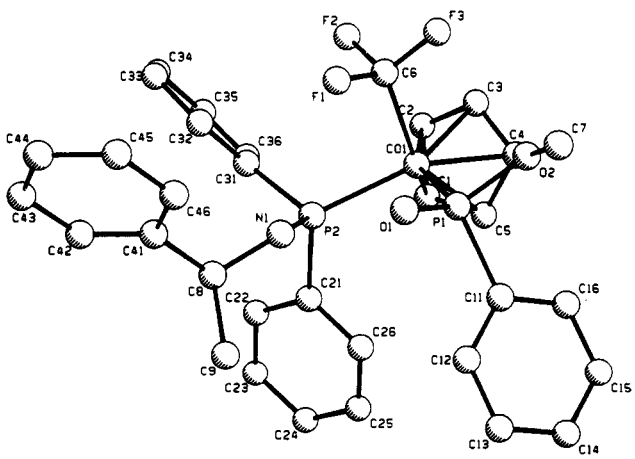

Figure 2. Structure of $[+4083]_{436}$-**3a**.

Mo Kα radiation except for $[+4083]_{436}$-(S_{Co};R_P;S_C)-**3a**, which was collected using a Cu Kα source. The CAD4 data were collected with profile analysis and ω–2θ scan mode. Rigaku data were collected a maximum of two rescans.

Structure Solution and Refinement. Orange prisms of $[-1325]_{436}$-(R_{Co};R_P;S_C)-**3a**, $[+4083]_{436}$-(S_{Co};R_P;S_C)-**3a**, and

(29) NRCCAD–An Enhanced CAD4 Control Program. Presented at the American Crystallography Association Annual Meeting, 1986, p 24.

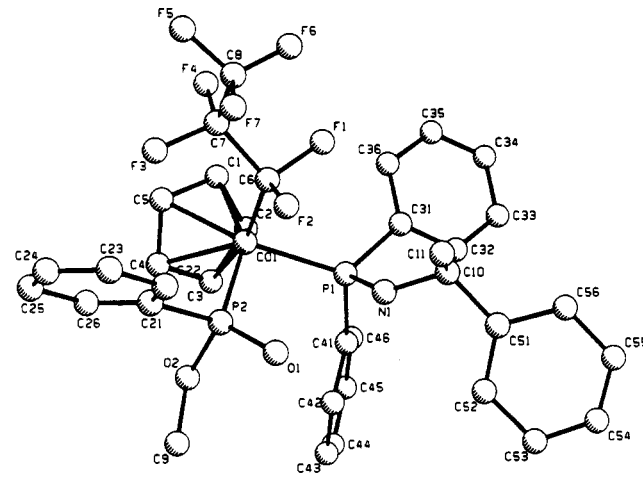

Figure 3. Structure of $[-2733]_{436}$-**3b**.

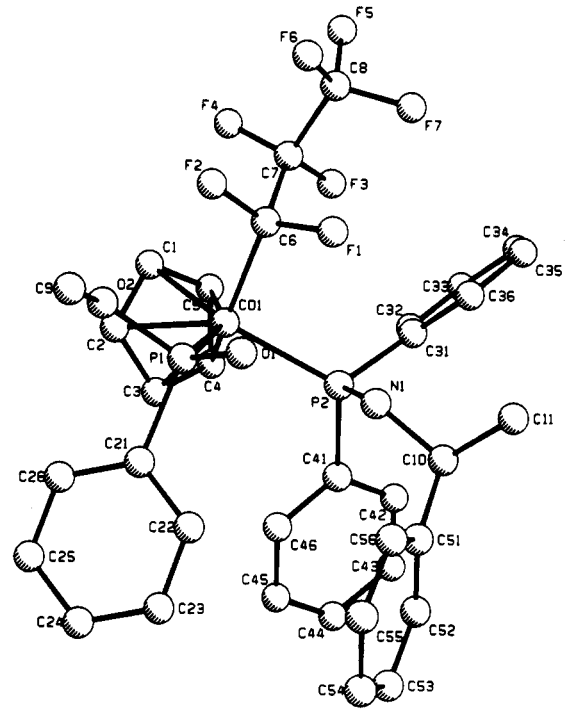

Figure 4. Structure of $[-1846]_{436}$-**3b**.

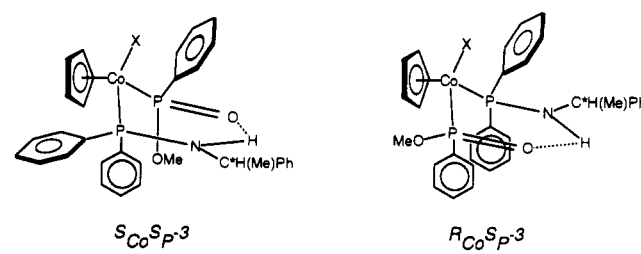

Figure 5. Solid-state conformation of **3**.

$[-2733]_{436}$-(R_{Co};R_P;S_C)-**3b** were grown by slow cooling of dilute ethyl acetate/hexane solutions of TLC-separated diastereomers at −30 °C. $[-1846]_{436}$-(R_{Co};S_P;S_C)-**3b** was recrystallized from methylene chloride/hexane solution at −30 °C. Trial structures were determined by direct methods with further refinements via successive cycles of least-squares and difference Fourier calculations using the NRCVAX suite of structure-solving programs[30] (CAD4 data) or Molecular Structure Corp.'s TEXSAN software package (Rigaku data). Limited significant data were obtained for $[-1325]_{436}$-(R_{Co};R_P;S_C)-**3a**, $[+4083]_{436}$-(S_{Co};R_P;S_C)-**3a**, and

(30) Gabe, E. J.; LePage, Y.; Charland, J. P.; Lee, F. L.; White, P. S. *J. Appl. Crystallogr.* **1989**, *22*, 384–387.

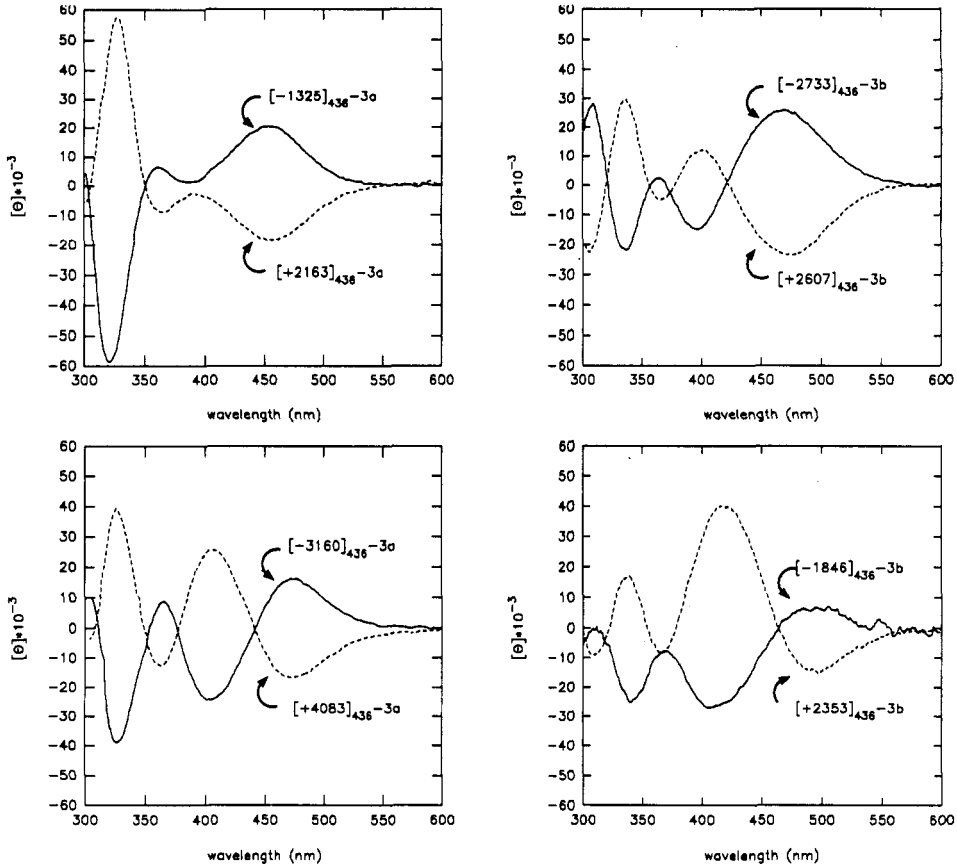

Figure 6. Circular dichroism spectra of **3a,b**.

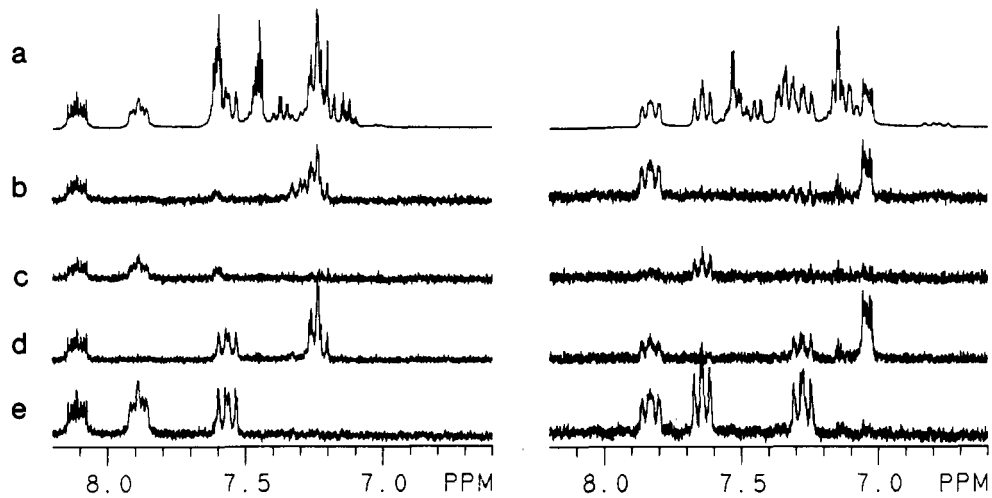

Figure 7. 300-MHz ^{1}H NOED difference spectra (aromatic region) for (S_{Co};S_P;S_O)-**3b** (left) and (R_{Co};S_P;S_O)-**3b** (right): (a) irradiation of η^5-Cp; (b) irradiation of C**H*; (c) irradiation of P–O*Me*; (d) irradiation of C**Me*; (e) ref 32.

[−1846]$_{436}$-(R_{Co};S_P;S_C)-**3b**; hence, all phenyls were refined as rigid groups. Hydrogen atoms were included at the calculated positions with B_{iso} values of 1.1 (CAD4 data) or 1.2 (Rigaku data) times those for the attached atoms and were not refined. Absolute configurations were determined using the NRCVAX utility BIVOET[31] ([−1325]$_{436}$-(R_{Co};R_P;S_C)-**3a** and [+4083]$_{436}$-(S_{Co};R_P;S_C)-**3a**) or by refinement of both enantiomers to convergence ([−1846]$_{436}$-(R_{Co};S_P;S_C)-**3b**). In each case the absolute configuration of carbon, originally derived from the natural chiral pool, was determined to be *S* in agreement with its known stereochemistry. For [−2733]$_{436}$-(R_{Co};R_P;S_C)-**3b** the stereochemical assignment assignment at Co and P was based on an assumed S absolute stereochemistry at the chiral carbon and confirmed by chiroptical data.

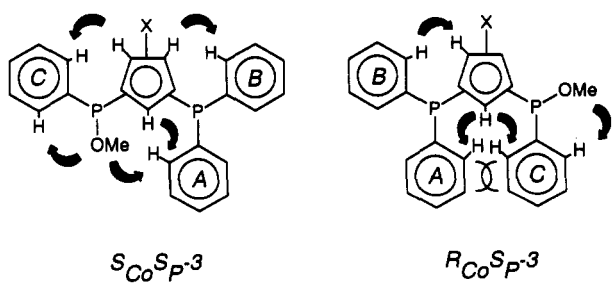

Figure 8. Nuclear Overhauser interactions for (S_{Co};S_P)-**3** (left) and (R_{Co};S_P)-**3** (right).

(31) LePage, Y.; Gabe, E. J.; Gainsford, G. J. *J. Appl. Crystallogr.* **1990**, *23*, 406–411.
(32) Walker, N.; Stuart, D. *Acta Crystallogr.* **1983**, *A39*, 158–166.

Table X. Kinetic Product Ratios[a]

compd	reacn	run no.	solvent	temp (°C)	% de $R_{Co};R_P/R_{Co};S_P$	% de $S_{Co};S_P/S_{Co};R_P$
3a	**1a** + $PPh(OMe)_2$	1	$CDCl_3$	30.0	26.7	29.5
3b	**1b** + $PPh(OMe)_2$	1	$CDCl_3$	30.0	44.3	45.8
		2	$CDCl_3$	30.0	46.0	46.3
		3	acetone	30.0	47.0	54 ± 8[b]
6a	**1a** + $PPh(OMe)_2$	1	$CDCl_3$	30.0	3.1[c]	
6b	**1b** + $PPh(OMe)_2$	1	$CDCl_3$	30.0	5.6[c]	
		2	$CDCl_3$		8.6[c]	

[a] Determined by integration of ^1H NMR spectra with ≤10% conversion to products. [b] Overlapping signal resulted in reduced precision. [c] Stereochemical assignment arbitrary.

Preparation of (η^5-Cp)Co*(X)(PPh(OMe)$_2$)(I) (4a,b). A solution of 115.0 mg (0.6765 mmol) of $PPh(OMe)_2$ in 5 mL of methylene chloride was added to a stirred solution of 265.7 mg (0.5931 mmol) of (η^5-Cp)Co(C_3F_7)(CO)I in 5 mL of the same solvent. The resulting clear orange solution was stirred for ca. 1 h. Removal of volatiles under oil pump vacuum left an orange, air-stable solid which was purified by chromatography on silica gel (CH_2Cl_2/hexane (1/1) elution) to give 210 mg (0.355 mmol, 60.0%) of **4b**. The CF_3 analog **4a** was prepared using the same procedure.

Preparation of (η^5-Cp)Co*(PPh$_2$NHC*H(Me)Ph)(X)(P*-(O)Ph(OMe)) (3a,b). Method A. In a typical preparation 43.7 mg (0.256 mmol) of $PPh(OMe)_2$ in ca. 20 mL of benzene was added via syringe to a solution of 185.4 mg (0.2556 mmol) of **1b** in ca. 20 mL of benzene and stirred under nitrogen at room temperature for 2 h. Removal of volatiles at oil pump vacuum left a dark solid which was purified by thick-layer radial chromatography on silica gel. Elution with 5/1 methylene chloride/ethyl acetate separated (in order of decreasing R_f values) a black zone containing unreacted **1b** and **4b** (102.4 mg) followed by two orange zones containing diastereomeric mixtures of **3b** (29.6 mg (15.4%) and 16.9 mg (8.8%)). Continued elution with 9/1 acetone/methanol separated an orange zone containing a 1/1 mixture of **6b** and free PNH* ligand (61 mg, 38% yield of **6b** after correction for displaced PNH*). Careful rechromatography of the orange zones containing **3b** using 4/1 ethyl acetate/hexane eluent separated four diastereomers which were purified by fractional crystallization from methylene chloride/hexane or ethyl acetate/hexane at −30 °C. Compound **3a** was obtained in an analogous manner; however, only the high R_f products were isolated and characterized. **3b** and **6b** could also be obtained by reacting **4b** with a stoichiometric amount of $PPh_2NHC(Me)Ph$ in benzene or acetone under similar conditions (method B).

Method C. A solution of 63.2 mg (0.207 mmol) of $PPh_2NHCH(Me)Ph$ in 20 mL of acetone was added dropwise to a solution prepared by dissolving 298.6 mg (0.4117 mmol) of **1b** and 121.8 mg (0.2064 mmol) of **4b** in ca. 20 mL of acetone. The dark reaction mixture was stirred for 2 h and worked up as described above to give 344.4 mg of recovered **1b** and **4b**, 69.5 mg (0.0922 mmol) of **3b**, and 5.1 mg (0.0082 mmol) of **6b** (14.7% and 1.3%, respectively, based on total Co).

Acknowledgment. We thank the Natural Sciences and Engineering Council of Canada (NSERC) and Memorial University for financial support.

OM920502O